Characterization of the ceramide moieties of sphingoglycolipids from mouse brain by ESI-MS/MS: identification of ceramides containing sphingadienine

Benoit Colsch,[*,†] Carlos Afonso,[†] Iuliana Popa,[§] Jacques Portoukalian,[§] Françoise Fournier,[†] Jean-Claude Tabet,[†] and Nicole Baumann[1,*]

Institut National de la Santé et de la Recherche Médicale U495,* Laboratoire de Neurochimie, Hopital de la Salpetriere, 75651 Paris cedex 13, France; Centre National de la Recherche Scientifique Unité Mixte de Recherche 7613,† Structure et Fonction de Molecules Bioactives, Universite Pierre et Marie Curie, 75252 Paris cedex 05, France; and Institut National de la Santé et de la Recherche Médicale U346,§ Laboratoire de Dermatologie, Hopital Edouard Herriot, 69003 Lyon, France

Abstract Sphingoglycolipids (SGLs) are cell membrane constituents. As the ceramide structure influences the biological properties of the SGL, we characterized by electrospray ionization tandem mass spectrometry the molecular species of ceramides present in SGL of mouse brain. We report here for the first time the presence in mammalian brain of sphingadienine (d18:2). Sphingenine (d18:1) is present in all SGL species, in contrast to eicosasphingenine (d20:1), which is a constituent of only gangliosides. Sphingadienine is present in galactosylceramide and sulfatides. Free ceramides contain the three types of bases. Thus, there could be two separate pools of free ceramides (d18:1, d18:2 and d20:1, d18:1) as precursors of complex SGL.— Colsch, B., C. Afonso, I. Popa, J. Portoukalian, F. Fournier, J-C. Tabet, and N. Baumann. **Characterization of the ceramide moieties of sphingoglycolipids from mouse brain by ESI-MS/MS: identification of ceramides containing sphingadienine. *J. Lipid Res.* 2004.** 45: **281–286.**

Supplementary key words ion trap • triple quadrupole • precursor ion scan • electrospray ionization tandem mass spectrometry

Sphingoglycolipids (SGLs) are cell membrane constituents especially enriched in the central nervous system. SGLs form specialized structures, mediate cell-cell and cell-substratum interactions, modulate the behavior of cellular proteins and receptors, and participate in signal transduction (1). They are synthesized de novo via a common backbone [sphinganine; DL-erythro-1,3-dihydroxy-2-aminooctadecane (d18:0)] that is modified to produce ceramides and more complex SGLs. Among the SGLs, gangliosides are mainly neuronal constituents; galactosylceramides (1-*O*-galactosyl-*N*-acylsphingosine) and sulfatides (galactosylceramide-I[3]-sulfate) are present in myelin and the glia myelin-forming cells (i.e., the oligodendrocyte) (2). Although the glycoepitope is known to be involved in the SGL properties, the ceramide structure is also implied, as it may influence the glycosylation pattern of the SGL (3), their presentation at the cell surface, and the degree of clustering of receptor molecules and the signaling pathways (3–5). Many studies have shown the complexity of the fatty acids present in the ceramide moiety of SGLs. Bovine brain gangliosides contain two major bases: sphingenine [d18:1; i.e., sphingosine (*trans*-D-erythro-2-amino-4-octadecene-1,3-diol)] and eicosasphingenine (d20:1) (6). Galactosylceramides and sulfatides contain only d18:1 sphingosine (7).

Mass spectrometry was widely used for the characterization of SGLs (8–14). These techniques readily discriminate between various forms of ceramides through: *i*) direct measurements of the molecular weights of native species and degradation products (15); and *ii*) selective dissociation of molecular species. We characterized by tandem mass spectrometry (16) combined with electrospray ionization (ESI) (17) the molecular species of ceramides present in gangliosides, sulfatides, galactosylceramides, and free ceramides of mouse brain. We report here for the first time the presence in mammalian brain of sphingadienine (d18:2), which has been described previously only in yeast (18), plants (19), human plasma (20), and erythrocyte membranes (21), as indicated by structural investigation.

MATERIALS AND METHODS

Sample preparation

Lipids were extracted from adult OF1 mouse brains and partitioned according to Folch, Lees, and Sloane (22). Gangliosides

Manuscript received 25 July 2003 and in revised form 29 October 2003.

Published, JLR Papers in Press, November 1, 2003.
DOI 10.1194/jlr.M300331-JLR200

[1] To whom correspondence should be addressed.
e-mail: baumann@ccr.jussieu.fr

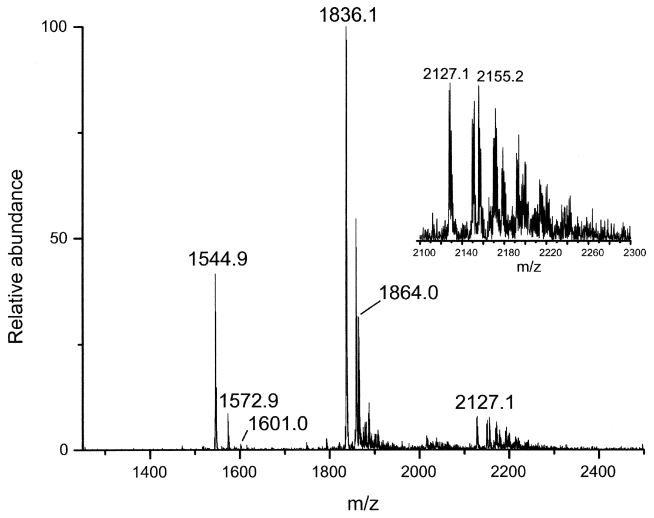

Fig. 1. Mass spectrum of gangliosides by electrospray ionization (ESI) ion-trap mass spectrometry in the negative ion mode. The main species are GM1 (*m/z* 1,544.9), GD1 (*m/z* 1,836.1), and GT1 (*m/z* 2,127.1) with C18:0 (d18:1) ceramide. The inset shows an enlargement of the spectrum for various species of GT1 that are present in the adult brain of mouse. Multiple cationized species are present especially in the case of GT1.

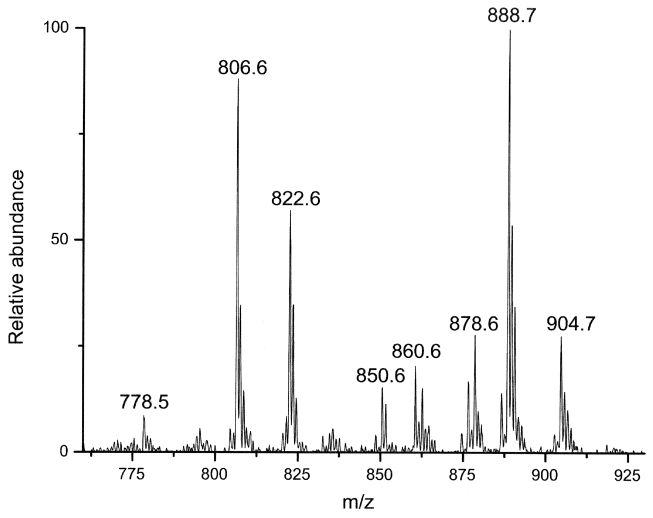

Fig. 2. ESI mass spectrum of sulfatides by ESI ion-trap mass spectrometry in the negative ion mode. Numerous sulfatide species were observed with two different sphingoid bases (d18:1 and d18:2) and fatty acids from C16:0 to C24:0(OH).

and sulfatides were enriched in the upper phase and desalted using C18:0-bonded silica gel columns (Supelco, l'Isle d'Abeau, France) according to Williams and McCluer (23).

Gangliosides and sulfatides recovered from the upper phase of partition were isolated by HPLC on a 250-4 Si100 column (Merck, Darmstadt, Germany) with a Hitachi L-6200 apparatus (Hialeah, FL) using a ternary gradient of hexane-isopropanol-water (55:36:9 to 55:30:15, v/v/v) at a flow rate 0.5 ml/min according to Peguet-Navarro et al. (24). Elution was monitored by TLC on silica gel 60 high-performance TLC plates (Merck) migrated in chloroform-methanol-water (60:35:8, v/v/v) along with standard sulfatides and gangliosides (Merck, Fontenay-sous-Bois, France). Free ceramides and native galactosylceramides were in the organic phase. The lower phase of partition was evaporated to dryness and taken up in chloroform. Free ceramides and galactosylceramides were purified using aminopropyl-bonded (LC-NH_2) silica gel cartridges (100 mg matrix; Supelco) according to Bodennec et al. (25). Free ceramides were hydrolyzed to release sphingoid bases under alkaline conditions according to Kadowaki and Grant (26).

Mass spectrometry

All products were analyzed using an ESI ion-trap instrument (27) (Esquire 3000; Bruker, Bremen, Germany) with a scan rate of 13,000 Th/s using a *m/z* range of 3,000 Th (ion ejection to β_z = 2:3). Both positive and negative modes were used. Sequential MS^nexperiments were performed under resonant excitation conditions. The automated ion charge control was set to 10,000 to avoid a space charge effect. The low mass cut-off used during the collision-induced dissociation (CID) experiments (related to the excitation at particular β_z values) was set automatically by the instrument software. Additional experiments were performed us-

TABLE 1. Ganglioside species characterized from the positive and negative electrospray ionization mass spectra of the upper phase fraction after HPLC purification

				Positive Ions				
	Negative Ions			Ceramide	Fatty Acid		Sphingoid Base	
Species	$[M-H]^-$	M	%[a]	$[M+H]^+$	$[M+H]^+$	Type	$[M+H-2H_2O]^+$	Type
GM1	1,544.9	1,545.9	81.1	564.5	282.3	C18:0	264.3	d18:1
	1,572.9	1,573.9	16.0	592.5	310.3	C20:0	264.3	d18:1
					282.3	C18:0	292.3	d20:1
	1,601.0	1,602.0	2.9	620.5	338.3	C22:0	264.3	d18:1
					310.3	C20:0	264.3	d20:1
GD1	1,836.1	1,837.1	57.6	564.5	282.3	C18:0	264.3	d18:1
	1,864.0	1,865.0	42.4	592.5	310.3	C20:0	264.3	d18:1
					282.3	C18:0	292.3	d20:1
GT1	2,127.1	2,128.1	46.8	564.5	282.3	C18:0	264.3	d18:1
	2,155.2	2,156.2	46.8	592.5	310.3	C20:0	264.3	d18:1
					282.3	C18:0	292.3	d20:1
	2,181.3	2,182.3	6.4	620.5	338.3	C22:0	264.3	d18:1
					310.3	C20:0	292.3	d20:1

[a] Values are calculated from the relative abundance determined from the negative ion molecular profile.

TABLE 2. Sulfatide species characterized from the positive and negative electrospray ionization mass spectra of the upper phase fraction after HPLC purification

Negative Ions			Positive Ions				
Sulfatide			Ceramide	Fatty Acid		Sphingoid Base	
$[M-H]^-$	M	%	$[M+H]^+$	$[M+H]^+$	Type	$[M+H-2H_2O]^+$	Type
778.5	779.5	1.9	538.5	256.3	C16:0	264.3	d18:1
804.5	805.5	0.3	564.5	282.3	C18:1	264.3	d18:1
				284.3	C18:0	262.3	d18:2
806.6	807.6	19.8	566.5	284.3	C18:0	264.3	d18:1
822.6	823.6	12.8	582.5	300.3	C18:0(OH)	264.3	d18:1
832.6	833.6	0.9	592.5	312.3	C20:0	262.3	d18:2
834.6	835.6	1.2	594.5	312.3	C20:0	264.3	d18:1
850.6	851.6	3.4	608.5	328.3	C20:0(OH)	262.3	d18:2
852.6	853.6	0.4	610.5	328.3	C20:0(OH)	264.3	d18:1
860.6	861.6	4.5	618.5	338.3	C22:1	262.3	d18:2
862.6	863.6	3.4	620.5	338.3	C22:1	264.3	d18:1
				340.4	C22:0	262.3	d18:2
864.6	865.6	1.5	622.5	340.4	C22:0	264.3	d18:1
874.6	875.6	0.9	634.5	352.4	C23:1	264.3	d18:1
				354.4	C23:0	262.3	d18:2
876.6	877.6	3.7	636.5	354.4	C23:0	264.3	d18:1
				356.4	C22:0(OH)	262.3	d18:2
878.6	879.6	6.3	638.5	356.4	C22:0(OH)	264.3	d18:1
886.6	887.6	3.1	646.5	366.4	C24:1	262.3	d18:2
888.7	889.7	22.6	648.5	366.4	C24:1	264.3	d18:1
				368.4	C24:0	262.3	d18:2
890.7	891.7	4.5	650.5	368.4	C24:0/C23:1(OH)	264.3	d18:1
				370.4	C23:0(OH)	262.3	d18:2
902.7	903.7	0.9	662.5	380.4	C25:1	264.3	d18:1
				382.4	C25:0/C24:1(OH)	262.3	d18:2
904.7	905.7	6.3	664.5	382.4	C25:0/C24:1(OH)	264.3	d18:1
				384.4	C24:0(OH)	262.3	d18:2
906.7	907.7	1.5	666.5	384.4	C24:0(OH)	264.3	d18:1

ing an ESI triple-quadrupole instrument (Micromass Quattro I, Manchester, UK) in the positive and precursor ion modes (28, 29). Argon was used as collision gas at a pressure of 3×10^{-4} mbar (cone voltage, 30 V; collision energy, 40 V).

RESULTS AND DISCUSSION

The Folch upper phase was analyzed by mass spectrometry after HPLC purification. **Figure 1** presents the ESI mass spectrum recorded in the negative ion mode. Several ion distributions centered around *m/z* 1,550, *m/z* 1,850, and *m/z* 2,150 are displayed that correspond to the deprotonated molecules of GM1 (II^3-α-*N*-acetylneuraminyl-gangliotetraglycosylceramide), GD1 (II^3-IV^3-α,α-di-*N*-acetylneuraminyl-gangliotetraglycosylceramide), and GT1 (II^3-α-*N*-acetylneuraminyl-α2→8-*N*-acetylneuraminyl-IV^3-α-*N*-acetylneuraminyl-gangliotetraglycosylceramide) gangliosides, respectively. It should be pointed out that much of the heterogeneity observed in the ESI mass spectrum, especially in the GT1 signal, is attributable to the existence of cationized species {e.g., $[M-(n+1)H+nNa]^-$}. Sequential MS^{n}experiments using the ion-trap mass spectrometer were carried

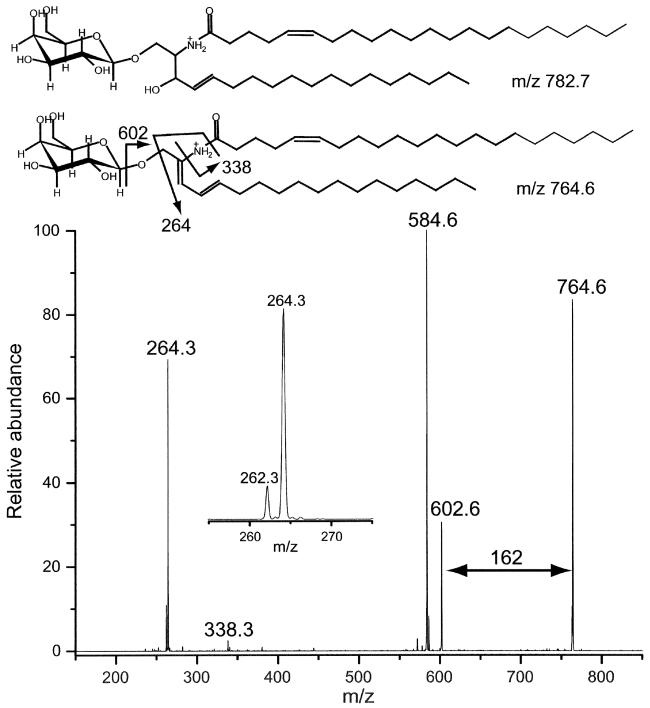

Fig. 3. Product ion scan of galactosylceramides (*m/z* 764.6) $[M+H-H_2O]^+$ from sulfatides after acid methanolysis by ESI ion-trap mass spectrometry in the positive mode. Top: Structure of a galactosylceramide with the various fragmentations obtained in the ion-trap instrument: *m/z* 264.3 represents d18:1, and *m/z* 602.6 represents the ceramide. Bottom: This spectrum indicates ceramide after the loss of the sugar moiety (neutral loss, 162 Da). The two sphingoid bases $[M+H-2H_2O]^+$ d18:1 (*m/z* 264.3) and d18:2 (*m/z* 262.3) were present along with the fatty acids to which they were associated: C22:1 (*m/z* 338.3) and C22:0 (*m/z* 340.3), respectively.

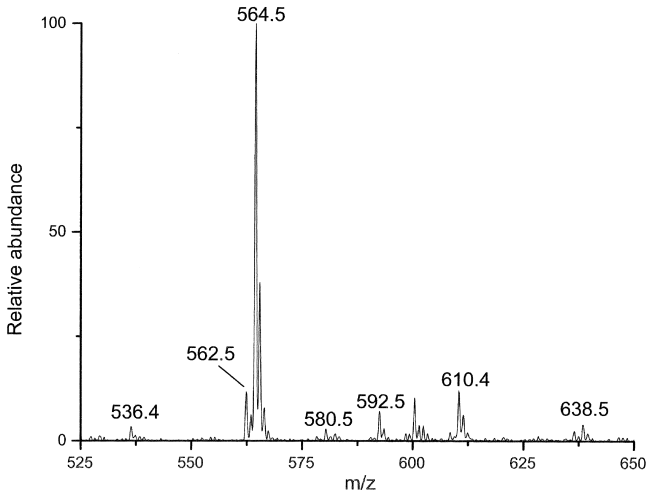

Fig. 4. Mass spectrum of free ceramides recorded on an ESI ion-trap instrument in the negative ion mode showing the diversity of the ceramide species.

out on these $[M - H]^-$ species, allowing confirmation of the sugar sequences (data not shown) and characterization of the ceramide moiety structure. Under these conditions, the sugars of the ganglio series and sialic acids are lost consecutively until the ceramide skeleton. The ceramide moiety was characterized using the positive ion mode from the sequential decomposition of the $[M + H]^+$ species. The detected species are reported in **Table 1** showing mainly d20:1 and d18:1 sphingoid bases, which are the same as in bovine brain (6), and C18:0, C20:0, and C22:0 as major fatty acid species.

Figure 2 represents the negative ion ESI mass spectrum of sulfatides obtained from the Folch upper phase. A high number of sulfatide species related to their ceramide composition were detected and are reported in **Table 2**. The relative abundance was obtained directly from this ESI mass spectrum. The major sulfatide species were d18:1 (C24:1) and d18:2 (C24:0) (*m/z* 888.7, 22.6%), d18:1 (C18:0) (*m/z* 806.6, 19.8%), and d18:1 [C18:0(OH)] (*m/z* 822.6, 12.8%). To obtain additional information, an acidic methanolysis (30) was performed allowing the conversion of the sulfatides to galactosylceramides, which are more efficiently ionized using the positive ion mode. Native galactosylceramides isolated from the Folch lower phase showed the same composition of ceramide species as native sulfatides (data not shown). This allowed, after sequential tandem mass spectrometry experiments, abundant fragment ions to be obtained that correspond to the

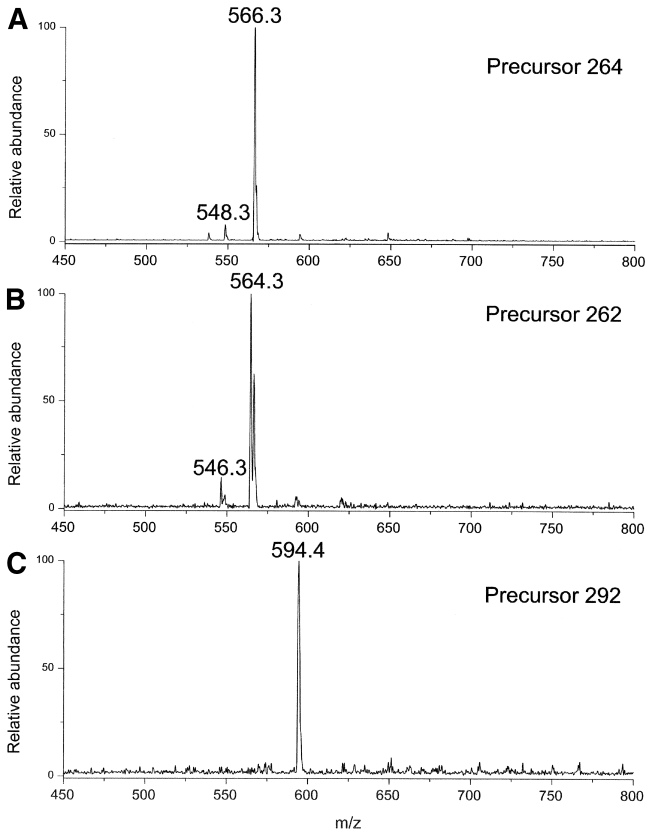

Fig. 5. Precursor ion scans (positive mode) of *m/z* 264 (d18:1) (A), *m/z* 262 (d18:2) (B), and *m/z* 292 (d20:1) (C) recorded using the ESI triple-quadrupole instrument showing specific ceramide profiles representing *m/z* 566.3, *m/z* 564.3, and *m/z* 594.4 precursor ions, respectively. The precursor ion scan of *m/z* 278 (d19:1) displayed no detectable signals (as expected).

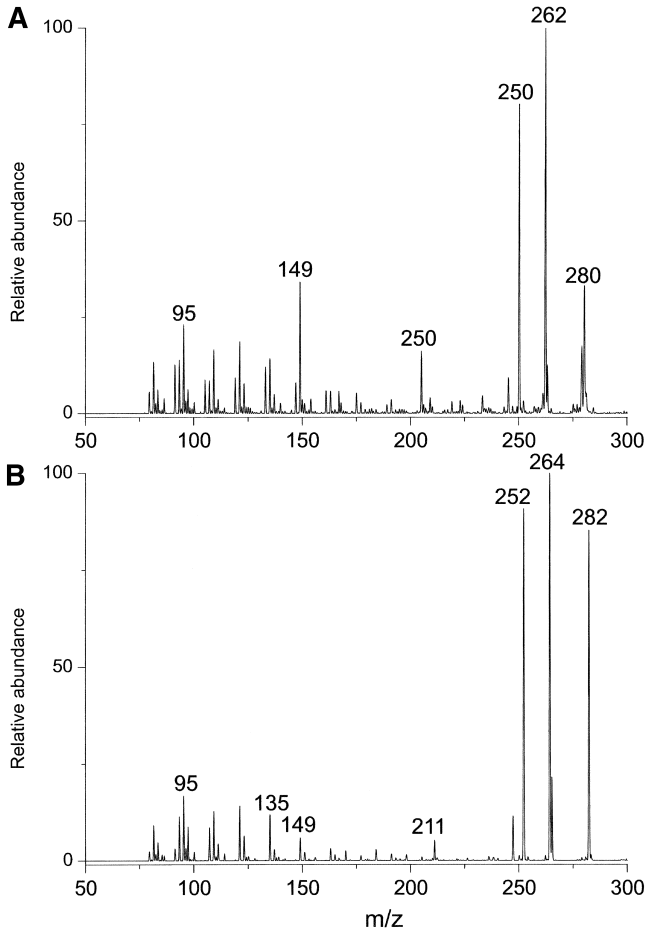

Fig. 6. Collision-induced dissociation spectrum of sphingoid bases (after alkaline hydrolysis) *m/z* 280 (d18:2) (A) and *m/z* 282 (d18:1) (B) displaying successive C-C bond cleavage.

sphingoid base $[M + H - 2H_2O]^+$ (**Fig. 3**). Under the declustering conditions used, dehydrated $[M + H - H_2O]^+$ ions were detected (*m/z* 764.6). Figure 3 shows the CID spectrum of *m/z* 764.6, which first lost the galactose to lead to the product ion *m/z* 602.6, corresponding to the ceramide moiety. These results confirmed what was observed with native sulfatide; furthermore, two complementary ions were detected at *m/z* 264.3 and *m/z* 338.3 (from the consecutive dissociation of *m/z* 602.6) attributed to protonated d18:1 sphingoid base and the protonated amide of the C22:1 fatty acid, respectively. A lesser signal at *m/z* 262.3 was also observed, together with a complementary *m/z* 340.3 ion. This observation can be rationalized by considering that the selected *m/z* 764.6 ion was a mixture of two isomeric ceramide species, C22:1 (d18:1) and C22:0 (d18:2). **Figure 4** represents a negative ion ESI mass spectrum of a mixture of different free ceramide species purified by LC-NH_2 columns from the Folch lower phase. Their fatty acid composition showed less diversity than ceramides obtained from galactosylceramides (data not shown) and sulfatides. The most abundant signal observed at *m/z* 564.5 in the negative mode is attributed to free ceramide C18:0 (d18:1). The *m/z* 562.5 peak represented ceramides with two sphingoid bases and two different fatty acids, C18:1 (d18:1) and C18:0 (d18:2), as shown by further fragmentation. We did not observe hydroxylated fatty acids under those experimental conditions. Most ions displayed in the ESI mass spectra were a mixture of isomers (Fig. 3), which makes interpretation difficult. To overcome this problem, precursor ion scan experiments under CID conditions were performed on the free ceramide sample using an ESI triple-quadrupole instrument operated in the positive ion mode. In this ionization mode, product ions corresponding to the sphingoid base (*m/z* 264 for d18:1) were displayed in high abundance. These species were monitored using the precursor ion mode. **Figure 5** shows the precursor ions of *m/z* 264.2, *m/z* 262.2, and *m/z* 292.2, corresponding to the sphingoid bases d18:1 (*m/z* 566.3), d18:2 (*m/z* 564.3), and d20:1 (*m/z* 594.4), respectively. As expected, no ceramide signal was detected from the precursor ion scan of *m/z* 278 (d19:1), which was performed as a control experiment. This technique allowed the detection in a single experiment of the ceramide species containing specifically the selected sphingoid base. **Figure 6** shows the fragmentation pattern of the sphingoid bases d18:1 and d18:2 obtained after alkaline hydrolysis according to Kadowaki and Grant (26). This confirms the great similarity between the two sphingoid bases. The localization of the second double bond has not yet been determined.

Sphingadienine (d18:2), first described in mammals in human plasma, represented 10% of the total sphingoid bases of mouse brain. The main base was sphingosine (d18:1), which represented 80% of the base content. Our results showed that sulfatides and galactosylceramides contain many ceramide species. This was attributable not only to the great variety of their fatty acid content [from C16:0 to C24:0(OH)] but also to their different sphingoid base species (d18:1 and d18:2). These two glycolipid species have the same ceramide distribution; this relates to the known fact that galactosylceramides are precursors of sulfatides. On the other hand, gangliosides contained fewer ceramide species (data not shown), and the base distribution was different, with a major content of sphingosine (d18:1) and the presence of eicosasphingenine (d20:1).

In free ceramides, the three types of sphingoid bases (d18:1, d18:2, and d20:1) have been found with a smaller variety of ceramides, as shown by the molecular profile. Thus, there seem to be two pools of free ceramides, one being precursors of galactosylceramides and sulfatides (d18:1 and d18:2), the other leading to the synthesis of gangliosides (d20:1 and d18:1).

The presence of sphingadienine in mouse brain, and probably in the brains of all mammals, leads to future research on this molecular species of ceramides in relation to its antigenic properties as well as its involvement in receptor function and cellular signaling.

REFERENCES

1. Merrill, A. H. 2002. De novo sphingolipid biosynthesis: a necessary, but dangerous, pathway. *J. Biol. Chem.* **277:** 25843–25846.
2. Baumann, N., and D. Pham-Dinh. 2001. Biology of oligodendrocyte and myelin in the mammalian central nervous system. *Physiol. Rev.* **81:** 871–927.
3. Hakomori, S. I. 2000. Traveling for the glycosphingolipid path. *Glycoconjugate J.* **17:** 627–647.
4. Gulbins, E., and G. Heike. 2002. Ceramide and cell death receptor clustering. *Biochim. Biophys. Acta.* **1585:** 139–145.
5. Venkataraman, K., and A. H. Futerman. 2000. Ceramide as a second messenger: sticky solutions to sticky problems. *Trends Cell Biol.* **10:** 408–412.
6. Ii, T., Y. Ohashi, and Y. Nagai. 1995. Structural elucidation of underivatized gangliosides by electrospray-ionization tandem mass spectrometry. *Carbohydr. Res.* **273:** 27–40.
7. Marbois, B. N., K. F. Faull, A. L. Fluharty, S. Raval-Fernandes, and L. H. Rome. 2000. Analysis of sulfatide from rat cerebellum and multiple sclerosis white matter by negative ion electrospray mass spectrometry. *Biochim. Biophys. Acta.* **1484:** 59–70.
8. Costello, C. E., P. Juhasz, and H. Perreault. 1994. New mass spectral approaches to ganglioside structure determinations. *Prog. Brain Res.* **101:** 45–61.
9. Domon, B., and C. E. Costello. 1988. Structure elucidation of glycosphingolipids and gangliosides using high-performance tandem mass spectrometry. *Biochemistry.* **27:** 1534–1543.
10. Costello, C. E., and J. E. Vath. 1990. Tandem mass spectrometry of glycolipids. *Methods Enzymol.* **193:** 738–768.
11. Sheeley, D. M., and V. N. Reinhold. 1998. Structural characterization of carbohydrate sequence, linkage, and branching in a quadrupole ion trap mass spectrometer: neutral oligosaccharides and N-linked glycans. *Anal. Chem.* **70:** 3053–3059.
12. Metelmann, W., Z. Vukelic, and J. Peter-Katalinic. 2001. Nano-electrospray ionization time-of-flight mass spectrometry of gangliosides from human brain tissue. *J. Mass Spectrom.* **36:** 21–29.
13. Ohashi, Y., R. Wang, R. Cotter, C. Fenselau, and Y. Nagai. 1987. Californium-252 plasma desorption mass spectrometry applied to saccharides and their conjugates. *Iyo Masu Kenkyukai Koenshu.* **12:** 189–192.
14. Sullards, M. C. 2000. Analysis of sphingomyelin, glucosylceramide, ceramide, sphingosine, and sphingosine 1-phosphate by tandem mass spectrometry. *Methods Enzymol.* **312:** 32–45.
15. Han, X. 2002. Characterization and direct quantification of ceramide molecular species from extracts of biological sample by electrospray ionization tandem mass spectrometry. *Anal. Biochem.* **302:** 199–212.

16. McLafferty, F. W. 1981. Tandem mass spectrometry. *Science.* **214:** 280–287.
17. Fenn, J. B., M. Mann, C. K. Meng, S. F. Wong, and C. M. Whitehouse. 1989. Electrospray ionization for mass spectrometry of large biomolecules. *Science.* **246:** 64–71.
18. Takakuwa, N., M. Kinoshita, Y. Oda, and M. Ohnishi. 2002. Existence of cerebroside in Saccharomyces kluyveri and its related species. *FEMS Yeast Res.* **2:** 533–538.
19. Imai, H., Y. Morimoto, and K. Tamura. 2000. Sphingoid base composition of monoglucosylceramide in Brassicaceae. *J. Plant Physiol.* **157:** 453–456.
20. Renkonen, O., and E. L. Hirvisalo. 1969. Structure of plasma sphingadienine. *J. Lipid Res.* **10:** 687–693.
21. Ando, S., M. Isobe, and Y. Nagai. 1976. High performance preparative column chromatography of lipids using a new porous silica, Iatrobeads. I. Separation of molecular species of sphingoglycolipids. *Biochim. Biophys. Acta.* **424:** 98–105.
22. Folch, J., M. Lees, and S. Sloane. 1957. A simple method for the isolation and purification of total lipid from animal tissues. *J. Biol. Chem.* **226:** 497–509.
23. Williams, M. A., and R. H. McCluer. 1980. The use of sep-pak C 18 cartridge during the isolation of gangliosides. *J. Neurochem.* **35:** 266–269.
24. Peguet-Navarro, J., M. Sportouch, I. Popa, O. Berthier, D. Schmitt, and J. Portoukalian. 2003. Gangliosides from human melanoma tumors impair dendritic cell differentiation from monocytes and induce their apoptosis. *J. Immunol.* **170:** 3488–3494.
25. Bodennec, J., O. Koul, I. Aguado, G. Brichon, G. Zwingelstein, and J. Portoukalian. 2000. A procedure for fractionation of sphingolipid classes by solid-phase extraction on aminopropyl cartridges. *J. Lipid Res.* **41:** 1524–1531.
26. Kadowaki, H., and M. A. Grant. 1994. Preparation of defined molecular species of lactosylceramide by chemical deacylation and reacylation with N-succinimidyl fatty acid esters. *Lipids.* **29:** 721–725.
27. March, R. E. 2000. Quadrupole ion trap mass spectrometry. A view at the turn of the century. *Int. J. Mass Spectrom.* **200:** 285–312.
28. Arnott, D. 2001. Basics of triple-stage quadrupole/ion-trap mass spectrometry: precursor, product and neutral-loss scanning. Electrospray ionization and nanospray ionization. *In* Proteome Research Mass Spectrometry. P. James, editor. Springer-Verlag, Germany. 11–31.
29. Hsu, F. F., A. Bohrer, and J. Turk. 1998. Electrospray ionization tandem mass spectrometric analysis of sulfatide. Determination of fragmentation patterns and characterization of molecular species expressed in brain and in pancreatic islets. *Biochim. Biophys. Acta.* **1392:** 202–216.
30. Karlsson, K. A., B. E. Samuelsson, and G. O. Steen. 1971. Lipid pattern and Na_K-dependent adenosine triphosphatase activity in the salt gland of duck before and after adaptation to hypertonic saline. *J. Membr. Biol.* **5:** 169–184.